JOURNAL OF COLLOID AND INTERFACE SCIENCE 172, 347–357 (1995)

Investigation of Alginate Binding to Germanium and Polystyrene Substrata Conditioned with Mussel Adhesive Protein

P. A. SUCI[1] AND G. G. GEESEY

Center for Biofilm Engineering, 409 Cobleigh Hall, Montana State University, Bozeman, Montana 59717

Received July 12, 1994; accepted January 3, 1995

Binding of alginate from *Macrocystis pyrifera* (kelp) to germanium and polystyrene substrata conditioned with mussel adhesive protein (MAP) from *Mytilis edulis*, to germanium substrata conditioned with bovine serum albumin (BSA) and polylysine, and to germanium substrata coated with aminopropyltriethoxysilane (APS) was investigated using attenuated total reflection Fourier transform infrared spectrometry. Binding of alginate to MAP appears to be proportional to surface coverage for levels tested. Distinct spectral features appear in the region associated with pyranose ring vibrations upon binding of alginate to MAP, polylysine, and APS, indicating that lysine residues play a prominent role in promoting irreversible adsorption with perturbation of pyranose ring atoms. BSA does not appear to enhance alginate adsorption over that observed on clean germanium and no new spectral features appear as a result of binding. The level of irreversible binding of alginate to germanium and polystyrene substrata conditioned with MAP is similar. © 1995 Academic Press, Inc.

Key Words: conditioning film; polysaccharide adsorption; alginate; mussel adhesive protein; attenuated total reflection Fourier transform infrared spectrometry.

1. INTRODUCTION

The manner in which adsorbed protein mediates cellular adhesion to substrata is relevant both to the events leading to thrombosis resulting from blood/materials interactions (1) and to microbial fouling of engineered surfaces placed in natural waters (2, 3). A "conditioning" film composed of adsorbed organic material has been found to form in a matter of minutes on materials exposed to marine waters (2–7). Therefore, fouling microorganisms typically encounter and attach to this modified substratum, rather than to the original pristine surface. In some cases the conditioning film has been shown to consist of a large proteinaceous component (2, 3).

Mature biofilms almost invariably consist of a matrix of extracellular polymeric substance (EPS) composed primarily of polysaccharides in which microorganisms are embedded (8–12). Two fundamental questions arise out of the assumption that the adhesive molecular interactions between the EPS and the underlying substratum are, in general, mediated by a conditioning film: (1) What are the molecular interactions involved? (2) Can these adhesive molecular interactions be modified by the underlying substratum properties?

Mussel adhesive proteins (MAP) are a component of the adhesive plaque with which *Mytilus edulis* anchors itself to materials having a wide variety of surface properties (13, 14). This plaque consists essentially of a fiber (collagen), a filler material (water), and a resin (MAP) (15). This "sticky" resin apparently forms bonds to both the surface and the fiber before a cross-linking reaction is catalyzed and this natural "composite thermoset" hardens. MAP promotes adhesion of a variety of cell types (16–18). For this purpose it is typically adsorbed from aqueous solution onto the intended substratum. A major component of MAP (mefp-1) is composed largely of tandem repeats of a decapeptide sequence. It is thought to have an open conformation with little secondary structure (19, 20). It is likely that these molecular characteristics contribute to its efficacy as a resin and may also contribute to its ability to promote cell adhesion. With MAP as a model conditioning film the questions posed above can be rephrased: (1) Which molecular properties are responsible for the stickiness of adsorbed MAP? (2) Can this stickiness be moderated or enhanced by properties of the underlying substratum?

For the present study MAP-conditioned substrata (germanium and polystyrene) were exposed to aqueous solutions of the polysaccharide, alginate, from *Macrocystis pyrifera* (kelp). For comparison, alginate binding to surfaces conditioned with polylysine and bovine serum albumin (BSA) was also investigated. Polylysine has been reported to enhance cell adhesion (21), while BSA is often used to block potential nonspecific binding sites, e.g., for immunological assays (22).

Alginate is a linear copolymer composed of the uronic acids α-L-guluronic and β-D-mannuronic acid (23). Alginate is the primary exopolysaccharide produced by *Pseudomonas aeruginosa* (24). Uronic acids constitute a significant fraction of the EPS of several marine pseudomonads (25, 26)

[1] To whom correspondence should be addressed.

0021-9797/95 $6.00

and, generally, are a common component of extracellular and cell surface polysaccharides of marine bacteria (27, 28). Strands of acidic polysaccharide have been observed connecting cells in biofilms to each other and to the substratum (9). Kelp alginate serves as a useful model compound for initial investigations of binding of acidic polysaccharides since it is relatively free of proteins and other organic components and is commercially available.

Attenuated total reflection Fourier transform infrared (ATR/FT-IR) spectrometry was used to investigate molecular bonding between alginate and the conditioned substrata. Adsorption of alginate onto germanium substrata conditioned with BSA, myoglobin, and β-lactoglobulin has been investigated previously using ATR/FT-IR (29).

2. MATERIALS AND METHODS

2.1. Materials

Mussel adhesive protein (freeze-dried) from *M. edulis* was purchased from Bioscience Laboratory (Floda, Sweden) and stored desiccated at −40°C. The amino acid composition according to the supplier is (per 1000 residues) 83 Asp, 74 Thr, 97 Ser, 64 Glu, 69 Pro, 132 Gly, 68 Ala, 50 Val, 25 Ile, 29 Leu, 30 Tyr, 12 Phe, 27 His, 115 Lys, 41 Arg, 41 Hyp, and 70 3,4-dihydroxy-L-phenylalanine (Dopa). Bovine serum albumin (Cat. No. A4503, MW 66 kDa), polylysine, hydrobromide (Cat. No. P1274, MW 132 kDa), and alginic acid, sodium salt (Cat. No. A2158, low viscosity) were from Sigma Chemical Co. (St. Louis, MO). The alginate contains less than 0.5% protein according to a Lowry assay with BSA as a standard (30). Total phosphorous (0.002%) and sulfur (0.06%) content of the alginate measured by inductively coupled plasma atomic absorption spectroscopy were provided by the vendor for the specific lot number. Aminopropyltriethoxysilane (APS) and polystyrene (MW 239,700) were from Aldrich Chemical Co. (Milwaukee, WI).

The buffer used for all experiments was Naval PS-1 synthetic seawater with omission of divalent cations and sulfate compounds and amended with $NaHCO_3$ to provide some buffering capacity in the neutral pH range (31). It consisted of (per liter water) 0.2 g KCl, 0.9 g KBr, 23 g NaCl, and 0.2 g $NaHCO_3$, pH 8.0 (adjusted with HCl). The omissions were intended to simplify the experimental conditions: sulfate absorbs quite strongly in the IR range of interest and divalent cations will cross-link alginate before it contacts the substratum. Water was ultrapure (Barnstead water purification system, Dubuque, IA). Ethyl alcohol, methanol, chloroform, and hexanes were HPLC grade (Aldrich Chemical Co.). Isopropyl alcohol was analytical grade (Fisher Scientific, Fairlawn, NJ).

2.2. Methods

2.2.1. Characterization of MAP. Polyacrylamide gel electrophoresis (5% acetic acid) indicated that the MAP preparation consisted of approximately 80% of the two Dopa-containing proteins of the resin: mefp-1 and -2, in equal quantities, and approximately 20% of two non-Dopa-containing proteins. The Coomassie blue-stained gel is shown in Fig. 1. Dopa-containing proteins were identified by two independent staining procedures: a redox-cycling reagent (32) and treatment with nitrous acid (33). The protocol for electrophoresis is described in detail elsewhere (34). Identification of bands originating from mefp-1 and -2 was based on previous assignments (35). The Dopa-containing protein, mefp-1, is reported to have a molecular weight of 130 kDa and to consist of a large fraction of tandem repeats of the decapeptide sequence: Ala–Lys–Pro–Ser–Tyr–Hyp–Hyp–Thr–Dopa–Lys (36).

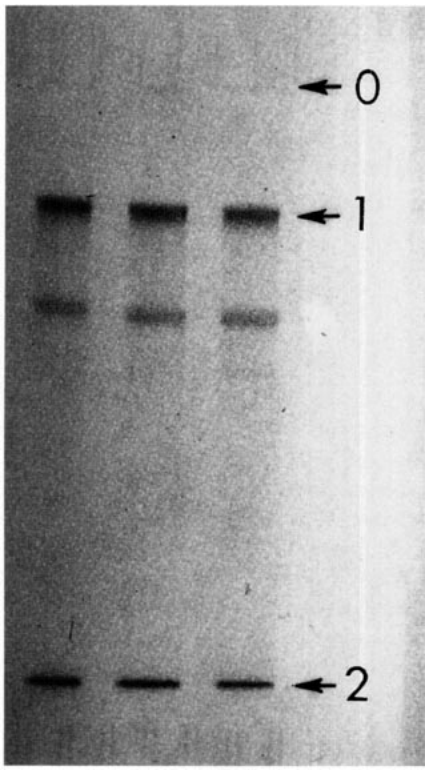

FIG. 1. Polyacrylamide gel of MAP stained with Coomassie blue. Arrows indicate (from top to bottom): gel origin, mefp-1, and mefp-2. The three lanes are replicates.

2.2.2. Surface preparation. Single crystal, cylindrical germanium internal reflection elements (IRE) (Spectra Tech, Stamford, CT) were cleaned by ultrasonication in a base bath (saturated KOH in isopropyl alcohol) for 10 min, followed by a series of rinses which all consisted of ultrasonication in various liquids for 10 min. Following the base bath were two rinses in ultrapure water followed by a gentle scrubbing with undiluted Micro cleaning solution using cotton swabs. The cleaning solution was flushed off in a hard stream of ultrapure water. The IRE was then subjected to the following rinses: ultrapure water (2×), ethyl alcohol,

and chloroform. This cleaning procedure removed adsorbed protein as indicated by disappearance of amide I and II bands, while degrading the throughput of the IRE minimally. Auger electron spectroscopy (Phi 595 scanning Auger microprobe) indicated that the elemental percentage composition of the first few monolayers of germanium substrata, cleaned by this protocol, was 9.11 ± 1.38 carbon, 6.51 ± 2.01 oxygen, and 83.92 ± 2.24 germanium.

2.2.3. Surface modification. Polystyrene was dip coated onto germanium IREs from a 2.0% solution of polystyrene in toluene (g/ml) at a speed of 0.5 cm/s. Film thickness estimated on the basis of a comparison of transmission spectra of films dip-coated onto germanium disks and polystyrene films of known thicknesses indicated that the films were approximately 0.1 μm thick with a reproducibility of ±10%. X-ray photoelectron spectroscopy (Surface Science Instruments, 600-μm diameter spot size, monochromatized aluminum $K\alpha$ source) of germanium disks, dip coated with polystyrene, indicated that the films were continuous (i.e., no germanium was detected). There was slight loss of the films during the course of the adsorption experiments as indicated by a decrease in the 1492 cm^{-1} IR line of the polystyrene film measured against air. This decrease was no more than 10% for experiments reported here and averaged 5.2%. In order to confirm that MAP-conditioning films were adsorbed primarily to the polystyrene films and not to any exposed germanium the following procedure was employed. After each experiment the IRE was sonicated for 10 min in toluene and then reinserted in the instrument and a spectrum was acquired in air. Previous tests showed that this sonication treatment removes all polystyrene from the IRE, as indicated by the disappearance of the associated IR bands, but does not diminish the amide II band of MAP bound directly to clean germanium. In no experiments was any residual amide II band found following sonication, indicating that adsorption of MAP was directly to the polystyrene.

For silanizing with APS the IRE was emersed in a 1% solution of APS in hexanes for 2 h in a nitrogen atmosphere at room temperature (approx. 25°C). The IRE was then rinsed in hexanes (1 min) and methanol (1 min) and air-dried for 1 h.

2.2.4. Adsorption protocol. For adsorption experiments the cylindrical IRE was positioned within a stainless steel flow chamber (Circle Cell, Spectra Tech). The interior cavity of the flow chamber is cylindrical with a diameter of 0.476 cm and a length of 2.7 cm. The volume contained in the annular region between the surface of the IRE and chamber wall is 0.289 cm^3. Fluid was introduced and displaced through entrance and exit ports at each end of the cavity. The IRE was held in place in the chamber by two Teflon O-rings.

A simple flow-through system was used to introduce protein, alginate, and synthetic seawater into the flow chamber. Teflon valves (Cole–Parmer, Niles, IL) served to shuttle the appropriate solution into tubing leading to the flow chamber. All tubing leading into the flow chamber as well as the fittings was Teflon (0.08 cm i.d.). Tubing was cleaned after each experiment by sonicating in base bath. The section of tubing connecting the reservoir containing protein to the flow chamber was made as short as possible (~20 cm). Effluent tubing was silicone. Fluid was pumped by threading this exit tubing through a peristaltic pump (Sage Instruments, Cambridge, MA) at 0.5 ml/min. All glassware was either acid cleaned (Nochromix (Godax Laboratories, New York) in concentrated H_2SO_4) or baked at 500°C for 3 h.

For experiments in which surfaces were conditioned with MAP the following protocol was followed: A 1 mg/ml stock solution of MAP was made in dilute HCl (pH 2.5) which had been deaerated by bubbling with N_2. The stock solution was stored at 5°C. A 3× concentrated solution of synthetic seawater was pH adjusted so that a 2:1 solution (dilute HCl:3× seawater) had a pH of 8.0. Immediately preceding each experiment the desired quantity of the stock solution was pipetted into dilute HCl (pH 2.5) to bring the volume to 0.67 ml in a small glass vial. Following this, 0.33 ml of the 3× seawater was added. This protocol approximates that prescribed for coating surfaces with a commercial preparation of MAP (Cell-Tak). For adsorption experiments involving BSA and polylysine stock solutions were made, and directly diluted with synthetic seawater. For all protein adsorption experiments a vial containing 1 ml of the desired concentration of protein was inserted into the flow system and the protein solution immediately pumped through a short section of leader tubing and through the flow chamber for 60 s. Flow was then stopped for 60 min to allow adsorption. Adsorption of protein was done under these static conditions to conserve MAP. Flow was then continued and the surface was exposed to the following sequence of solutions: seawater (60 min), 10 mg/ml alginate seawater solution, pH 8.0 (30 min), and again seawater (120 min). For adsorption of alginate onto the IRE coated with APS, 10 mg/ml alginate in ultrapure water was adsorbed for 30 min at 0.5 ml/min flow rate and then rinsed with flowing ultrapure water for 120 min.

2.2.5. FT-IR spectrometry. During the course of each experiment infrared spectra were acquired every 5 min. A Perkin–Elmer Model 1800 Fourier transform infrared spectrophotometer equipped with a liquid N_2-cooled, medium-range mercury–cadmium telluride detector (5000–580 cm^{-1}) was used to collect the FT-IR spectra. Interferograms were double sided, apodization was a weak Beer–Norton function, and the range was 4000–700 cm^{-1} with an interval of 1 cm^{-1} and nominal resolution of 2 cm^{-1}; 50 interferograms were averaged per spectrum; water vapor bands were removed by subtraction of a pure water vapor spectrum. Fluctuations in intensity of the strong water band at 1640

cm^{-1} resulted in appearance of this band in the difference spectra. This residual water adsorption band was removed by subtracting out a pure water spectrum using the ratio of areas of the absorption water band centered at 2120 cm^{-1} as a normalization factor (37). Variation in absorbance values resulting from slight differences in alignment of the flow chamber on the optical bench and coating with polystyrene films was normalized by using the area of the water absorption band at 1640 cm^{-1} (area, 1540 to 1740 cm^{-1}) as an internal standard (38). Areas of spectral features were computed for the region bounded by the data curve and by a linear baseline drawn between the two endpoints of the integration. Theoretical descriptions of the evanescent field which penetrates from the surface of the IRE in the attenuated total reflection geometry are available (39). Briefly, for a 45° incident angle, the evanescent field intensity decreases exponentially with distance from the IRE surface such that 95% of the energy is contained within 0.477 μm of a germanium–water interface at 2000 cm^{-1} and within 1.05 μm at 900 cm^{-1}. FT-IR measurements were made in a temperature-controlled room (20 ± 0.5°C).

Transmission spectra were measured in a 15-μm pathlength demountable cell with calcium fluoride windows (Spectra Tech).

2.2.6. Estimation of the surface density of lysine residues of adsorbed protein films. Protein surface coverage was estimated based on area of the amide II band using published correlations. Adsorption conditions of Fink *et al.* (38) resemble those here (saline solution, pH 7.4 on germanium). Extinction coefficients for solution phase BSA compare favorably with our estimates (within 80%). Fink *et al.* obtained correlations for adsorbed human albumin, immunoglobulin, and fibrinogen. Using their data, a factor for conversion of amide II areas to surface coverage in $\mu g/cm^2$ can be estimated. This conversion factor is 0.26 ± 0.12 $\mu g/cm^2$ per unit area amide II (abs · cm^{-1}). In order to convert protein surface coverage to lysine residue surface density the amino acid composition of the MAP provided by the supplier was used.

3. RESULTS

A small but measurable amount of alginate is retained on clean germanium following a 30-min exposure to a 10 mg/ml solution followed by a 120-min rinse with synthetic seawater. Spectra acquired immediately before the rinse and after the 120-min rinse are displayed in Fig. 2. The boxed-in region contains resonance frequencies associated with the pyranose ring. Binding to the surface has been quantified by computing areas of the prominent band at 1034 cm^{-1} (integration limits, 1070 to 1000 cm^{-1}), which will be referred to as "algI." The time course of changes in this band, reflecting the appearance of alginate in the interfacial region of the germanium IRE, followed by diffusion and

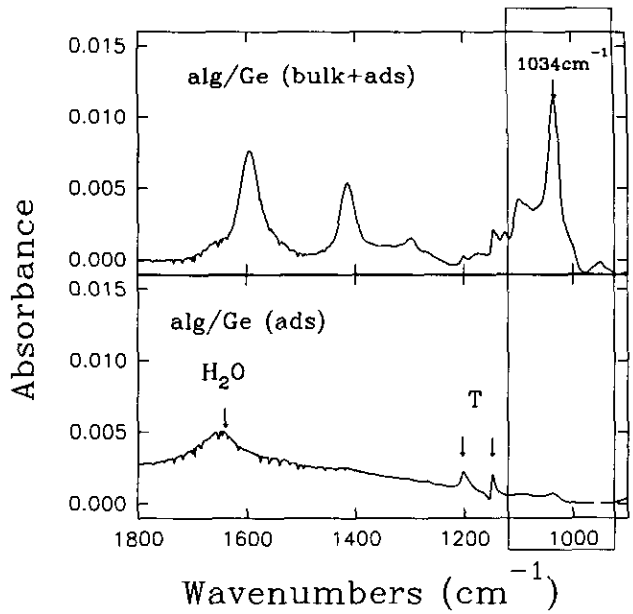

FIG. 2. ATR/FT-IR spectra obtained during exposure of clean germanium to 10 mg/ml alginate and the rinse period. Top, immediately before the rinse with seawater; bottom, after a 120-min rinse with seawater. Bands associated with residual water (H_2O) and with the Teflon O-rings (T) are indicated.

desorption from the interface during the rinse period, is shown in Fig. 3a.

If 10 min is allowed for diffusion of solution phase alginate from the interfacial region, the desorption curve can be analyzed by assuming that the adsorbed portion consists of two components: a "reversibly" adsorbed component which desorbs with first-order kinetics and an "irreversibly" adsorbed component which is retained indefinitely (29). Letting c_2 represent the irreversibly adsorbed component, one obtains

$$D(t) = c_1 \exp(-t/\tau) + c_2. \quad [1]$$

The symbol $D(t)$ stands for data at time t (ordinate value of the data point), τ is the time constant for the first-order desorption, and c_1 is a fitting parameter. At long times $D(t)$ approaches an ordinate value of c_2. Figure 3b presents the linear fit to $\ln(D(t) - c_2)$, where c_2 is obtained from the nonlinear fit (Sigma Plot) of Eq. [1] to the desorption data 10 min after the rinse with seawater is initiated, and "ln" is the natural log. The correlation coefficient for the linear fit is 0.987. The estimate for τ is 19.6 min.

In order to see whether MAP-conditioning films enhance irreversible adsorption of alginate (as defined above) we have prepared germanium substrata with increasing surface coverages of MAP and measured the alginate irreversibly adsorbed to each of these conditioned surfaces. A spectrum of adsorbed MAP is shown in Fig. 4. The amide I and II

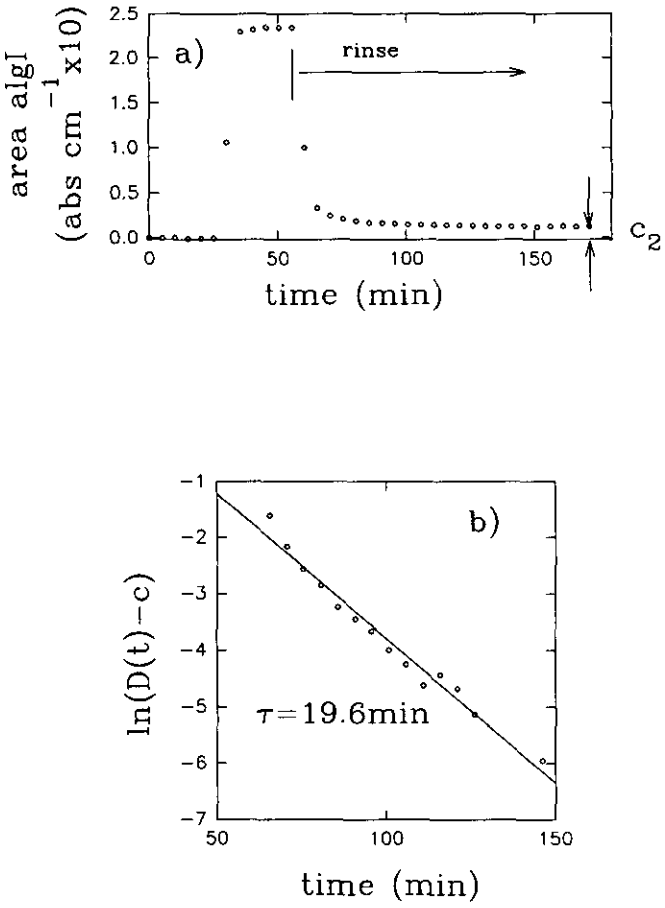

FIG. 3. (a) Change in area of the alginate band centered at 1034 cm^{-1} (algI) versus time. (b) Semi-log plot of alginate desorption according to Eq. [1] (see text). Times on abscissa are as in (a).

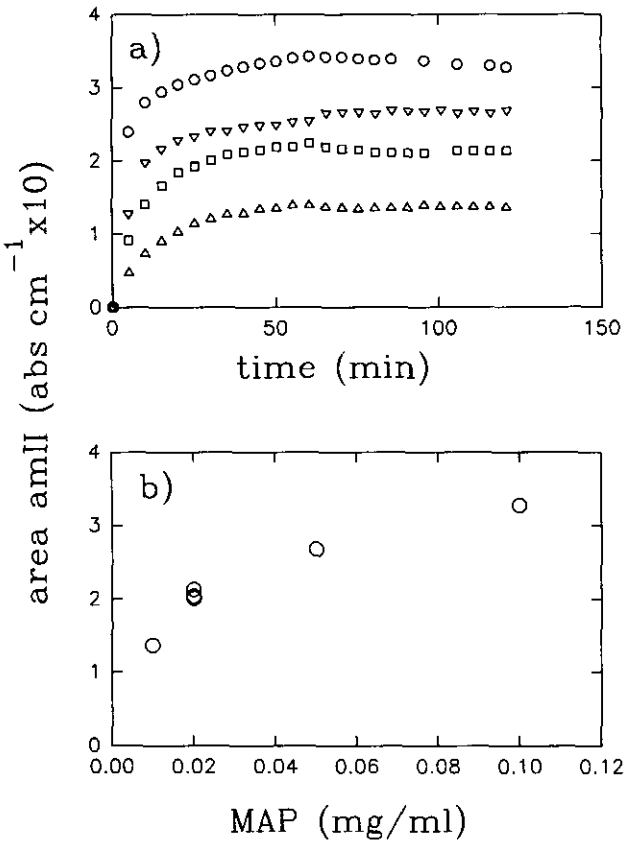

FIG. 5. (a) Time course of MAP adsorption on clean germanium monitored by area of the amide II (amII) band for four MAP bulk concentrations: △, 1.0 mg/ml; □, 0.02 mg/ml; ▽, 0.05 mg/ml; ○, 0.1 mg/ml. (b) MAP binding curve on germanium (for 0.02 mg/ml MAP the experiment was repeated three times).

bands typical of proteins are evident. In addition, some features which are less typical of proteins are indicated. The wide asymmetrical band at 1256 cm^{-1} has been observed previously in IR spectra of MAP and assigned to the Dopa

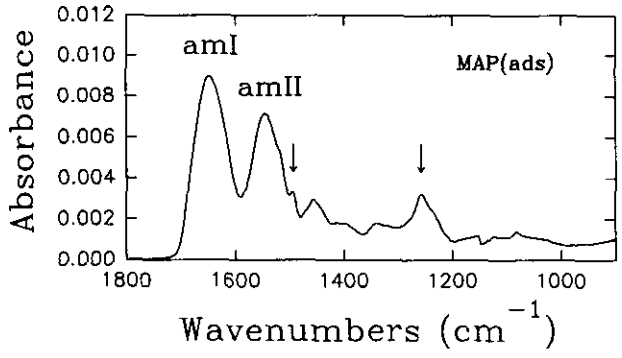

FIG. 4. FT-IR spectrum of MAP adsorbed to clean germanium at the end of the 120-min rinse period. Amide I (amI) and II (amII) bands are indicated as well as spectral features somewhat atypical of proteins (arrows).

residues (40, 41). Figure 5a presents the time course for adsorption/desorption of MAP onto the IRE (MAP) for four bulk concentrations (0.01, 0.02, 0.05, and 0.10 mg/ml). The ordinate values were computed as areas of the amide II band from 1591 to 1478 cm^{-1}. Very little change in amide II absorbance occurs after the adsorbed MAP is exposed to flowing seawater at 60 min, indicating that the MAP is irreversibly bound to the germanium surface. (Also the absorbance from the bulk MAP component appears to be negligible). Desorption curves for BSA adsorbed onto germanium appear similar. Figure 5b is the binding curve for MAP on germanium obtained by plotting the amide II areas after the 60-min rinse period versus the bulk MAP concentration.

Following conditioning with MAP or BSA, the IREs were exposed to alginate and rinsed with synthetic seawater. During this period no change in amide bands of the underlying protein was observed, indicating that desorption of the conditioning film was negligible. Difference spectra calculated between the last protein spectrum acquired before introduction of alginate and subsequent spectra reveal an increase in distinctive bands from the alginate followed by an abrupt

TABLE 1
Time Constants and Plateau Values[a] for Alginate Desorption from MAP- and BSA-Conditioned Surfaces

Protein	C (mg/ml)[b]	τ (min)	c_2	R^2
MAP	0.01	14.9	0.152	0.932
	0.02	22.7	0.264	0.991
	0.02	20.4	0.282	0.955
	0.02	24.4	0.347	0.831
	0.05	20.4	0.378	0.961
	0.1	14.7	0.551	0.971
BSA	0.02	31.3	0.112	0.929
	0.05	21.7	0.079	0.963
	0.1	32.3	0.153	0.853
	0.1	27.0	0.106	0.945
	0.1	30.3	0.033	0.963
	0.1	10.7	0.009	0.966
None	0	28.6	0.077	0.930
	0	19.6	0.132	0.987

[a] Parameter fits to Eq. [1].
[b] Concentration of bulk protein.

decrease as the surface is rinsed with seawater. In terms of general shape, the time courses based on areas computed over the interval from 1070 to 1000 cm^{-1} appear almost identical to the time course presented in Fig. 3a. (In the case of MAP-conditioned surfaces, the band structure in the pyranose ring region has been altered as described below). Desorption curves were analyzed as described above using Eq. [1]. Results of fitting parameters τ and c_2 in Eq. [1] for alginate adsorption onto clean germanium and germanium conditioned with MAP and BSA are summarized in Table 1 and Fig. 6. According to this analysis, conditioning with MAP appears to enhance adsorption of alginate, while levels of alginate retained on BSA-conditioned surfaces are approximately the same as those retained on clean germanium.

Spectral features in the pyranose ring region of the alginate retained on clean germanium and on BSA-conditioned germanium appear similar to features of the transmission spectrum of bulk solution phase alginate (Figs. 7a–7c). However, for MAP-conditioned germanium the spectral features of this bound alginate are altered (Fig. 7d). Specifically, the prominent band at 1034 cm^{-1} which is associated with C–O stretches of the pyranose ring of alginate appears to split into bands centered at 1030 and 1054 cm^{-1}. The limits of integration used for computation of the 1034 cm^{-1} band above have included this entire larger spectral feature, referred to as "algI" (see Fig. 7d). In addition, a band centered at 965 cm^{-1} and a wide band between 1200 and 1300 cm^{-1} (Fig. 8a) appear. These features resemble closely those for the adsorbed component retained on germanium conditioned with polylysine (Fig. 8b) and APS-coated germanium (Fig. 8c). If the area of algI is plotted against the estimated density of lysine residues for MAP and polylysine-conditioned surfaces the resulting curve increases monotonically (Fig. 9). The density of lysine residues was estimated as described under Materials and Methods.

The spectral feature indicated as "agII" in Fig. 7d exhibits very little decrease after flowing seawater is reintroduced into the chamber (Fig. 10), implying that this spectral feature originates specifically from a molecular interaction with the MAP-conditioned substratum which is associated with irreversible binding. The algII band is relatively isolated from other alginate spectral features and from bands of polystyrene. Thus, this spectral feature can be used effectively to compare the influence of the underlying substratum (polystyrene vs germanium) on the strength of the interaction of alginate with MAP-conditioned surfaces. Figure 11 displays areas of the algII band vs MAP surface coverage (area of the amide II band) for polystyrene and germanium. Although the slope of the regression line for the polystyrene surface is slightly greater, it is obvious that the slopes for polystyrene

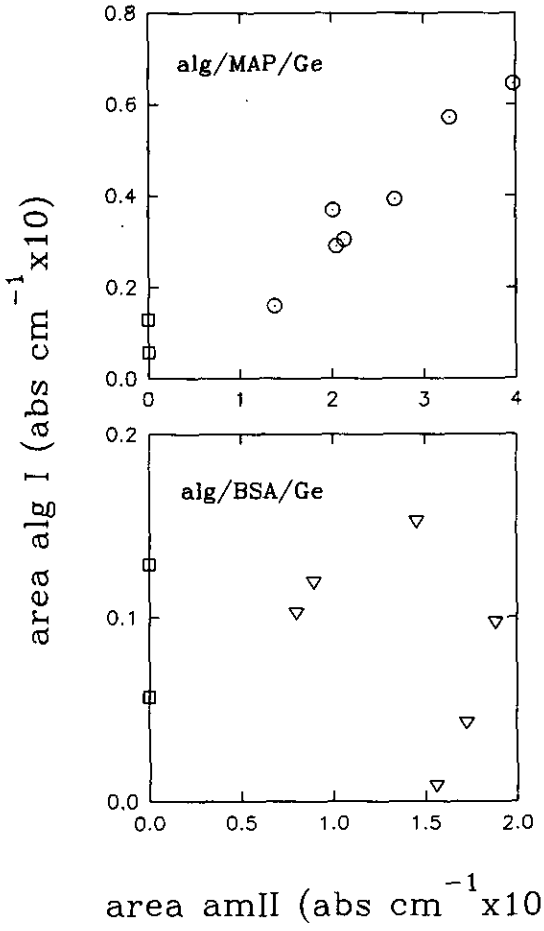

FIG. 6. Area of the alginate spectral feature algI versus protein surface coverage, i.e., area of amII. Top, germanium conditioned with MAP; bottom, germanium conditioned with BSA. The largest surface coverage of MAP presented in the top was obtained by adsorption from a 0.01 mg/ml MAP bulk solution followed by adsorption from a 0.05 mg/ml MAP bulk solution.

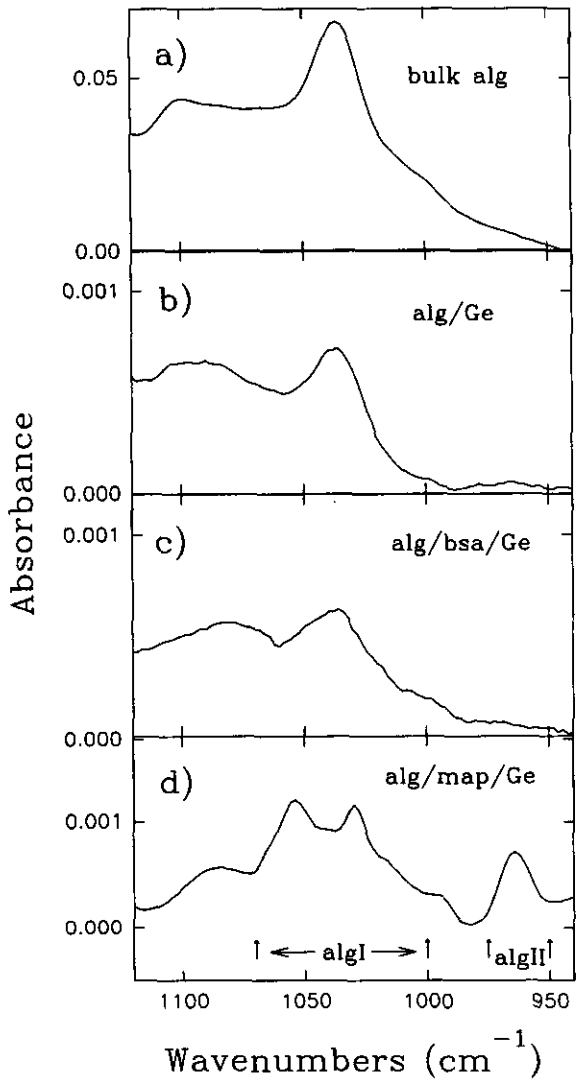

FIG. 7. FT-IR spectra of pyranose ring C–O stretch region. (a) Transmission spectrum of bulk solution alginate; (b, c, d) ATR spectra of alginate retained after the 120-min rinse period on (b) clean germanium, (c) germanium conditioned with BSA, and (d) germanium conditioned with MAP.

and germanium will overlap within the 95% confidence intervals.

In bulk solution, alginate reacts with equimolar concentrations of polylysine (10 mg/ml in synthetic seawater, pH 8.0), forming a white fibrous precipitate. When the pH is raised above 12.5 this precipitate disappears. If the pH is lowered below 9.0 within 5 min, the mixture again becomes cloudy. Transmission spectra of this white precipitate contain a prominent band centered at 950 cm^{-1} which is not present in the transmission spectrum of bulk alginate (Fig. 8d). However, other spectral features which are prominent in adsorbed components of alginate on MAP, polylysine, and APS (Figs. 7a–7c), namely the shoulder at 1054 cm^{-1} and the wide band between 1200 and 1300 cm^{-1}, are not evident.

4. DISCUSSION

4.1. Adsorption of Alginate onto MAP-Conditioned Germanium: Nature of the Bonding Interaction

MAP appears to enhance irreversible adsorption of alginate onto germanium. This is indicated by the increase in spectral features associated with pyranose ring vibrations of alginate as MAP surface coverage is increased (Fig. 6). Moreover, this enhancement of alginate adsorption appears to be nearly proportional to MAP surface coverage. In contrast, conditioning the surface with BSA does not increase alginate adsorption above the level adsorbed onto clean ger-

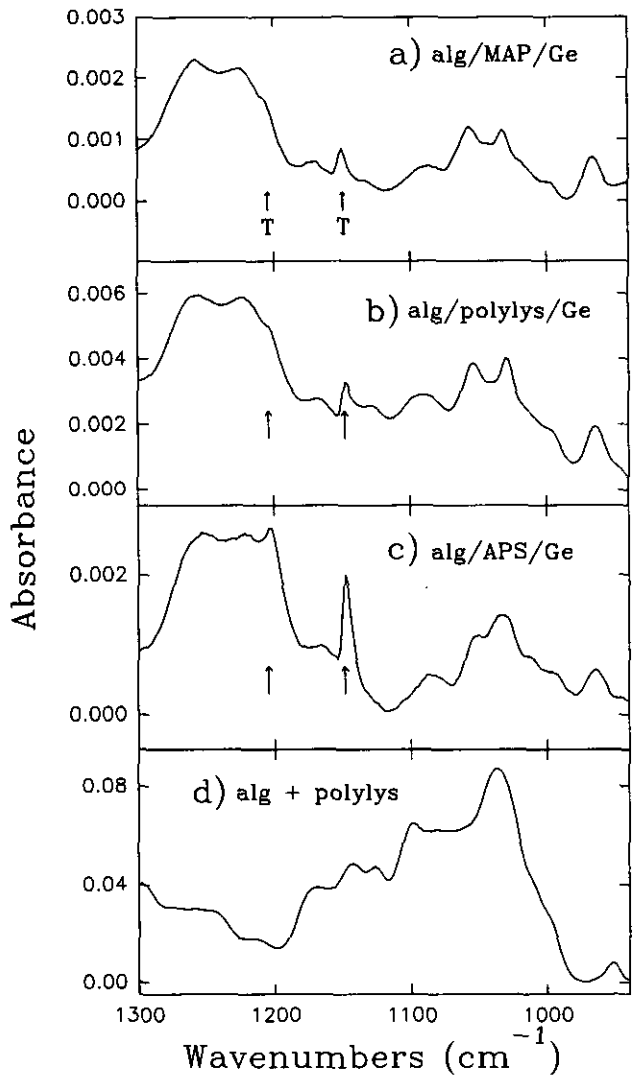

FIG. 8. FT-IR spectra of alginate binding to molecules incorporating amine groups: (a, b, c) ATR spectra of alginate retained after the 120-min rinse period on germanium conditioned with (a) MAP, (b) polylysine, (c) germanium coated with APS; (d) transmission spectrum of the precipitate formed upon mixing equimolar concentrations of alginate and polylysine. Positions of bands originating from the Teflon O-rings are indicated by arrows in ATR spectra.

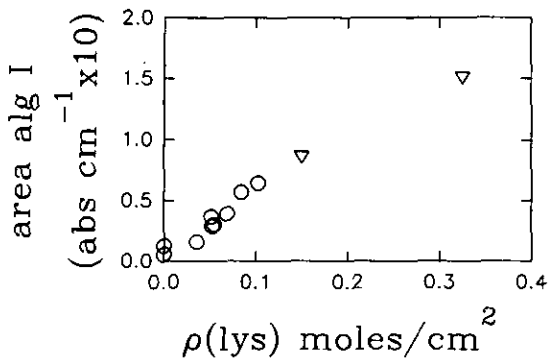

FIG. 9. Area of the alginate spectral feature algI versus estimated density of polylysine residues in mol/cm^2 for germanium conditioned with MAP (○), and with polylysine (▽).

manium. This suggests that the molecular interactions between MAP and alginate at the interface belong in a special class which one could identify as adhesive interactions between protein-conditioning films and polysaccharides.

The molecular bonding between MAP and alginate at the interface appears to be qualitatively different from bonding which promotes irreversible binding of alginate to clean germanium and BSA-conditioned germanium. Distinct spectral features appear in the C–O stretch region of the pyranose ring when germanium substrata conditioned with MAP are exposed to alginate (Fig. 8a). These features are not evident in transmission spectra of bulk solution alginate or the small amount of alginate retained on clean germanium or BSA-conditioned germanium after the 120-min rinse period (Fig. 7). A wide band between 1200 and 1300 cm^{-1} also appears when germanium conditioned with MAP is exposed to alginate (Fig. 8a). Although this wide band overlaps with a prominent spectral feature of MAP (Fig. 4), it apparently is not an enhancement of IR resonances originating directly from a unique molecular component of the MAP (see below).

Spectral features which appear when germanium substrata conditioned with polylysine are exposed to alginate closely resemble those produced by interaction of alginate with adsorbed MAP (Fig. 8). Therefore, it seems likely that the molecular interactions responsible for this irreversible binding to MAP involve predominantly lysine residues. This hypothesis is supported by data presented in Fig. 9 showing that the interaction between alginate and conditioned substrata appears to increase monotonically with increased density of lysine residues. Furthermore, contribution of the peptide linkage to this interaction may be minimal, since similar spectral features are produced by binding of alginate to propylamine groups grafted to the germanium substrate via siloxane bonds (APS) (Fig. 8c).

Nearly all carbohydrates and polysaccharides exhibit strong IR absorbance bands in the region from ~1120 to 900 cm^{-1} (42). Vibrations in this region have been variously assigned to C–O–H deformations (42), C–O stretch (29), and a combination of C–O and C–O–H stretching (43). Theoretical calculations lead to the interpretation that vibrations in this region originate from many coupled vibrations of the pyranose ring (42). Thus, it seems plausible that the apparent "splitting" of the alginate band at 1034 cm^{-1} into bands centered at 1054 and 1030 cm^{-1} and the appearance of the band at 965 cm^{-1} all derive from perturbation of the pyranose ring vibrations. It seems unlikely that this is caused purely by a simple ionic bond between the carboxylate functionalities and the protonated lysine residues. It may be that the negatively charged alginate is being driven to the surface by the positive charge conferred by the lysine residues, facilitating formation of other bonds (inter- or intramolecular H bonds, or van der Waals interactions). The isoelectric pH of MAP is greater than 10 (44), while that of BSA is 4.8 (45). Therefore, even though BSA is relatively densely packed with lysine residues (76/1000), its overall charge is negative at pH 8.0. This may explain its relatively nonadhesive character in the present context.

The interpretation of the spectral feature which appears between 1200 and 1300 cm^{-1} upon interaction of alginate with MAP-conditioned germanium is not straightforward. Since this wide band appears for binding of alginate to the APS-coated surface which contains no peptide linkages one can eliminate an enhancement of amide III resonances from consideration. Resonant frequencies in the range 1200 to 1300 cm^{-1} appear in polysaccharides which incorporate monosaccharides containing pyranose rings, e.g., crystalline amylose (42). Thus, it may be that resonant frequencies in this region are being enhanced by intramolecular H bonding between alginate sugar units which is promoted or facilitated by the initial electrostatically driven adsorption to the conditioned substrata. It is also possible that the observed spectral changes resulting from alginate adsorption onto the MAP,

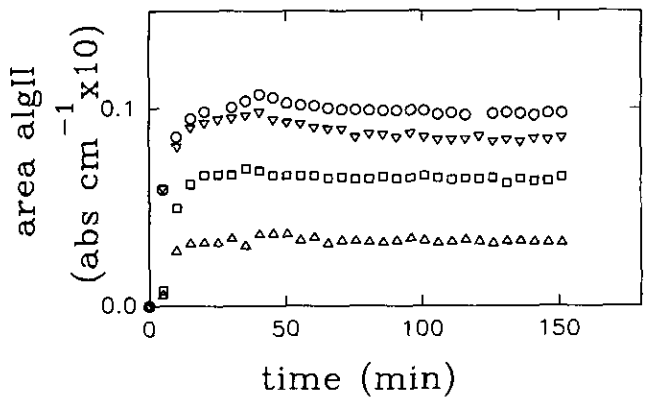

FIG. 10. Area of the alginate band algII versus time during exposure of MAP-conditioned germanium to 10 mg/ml alginate and the 120-min rinse period. Increasing MAP surface coverages were produced by conditioning with increasing bulk MAP concentrations as in Fig. 5: △, 0.01 mg/ml; □, 0.02 mg/ml; ▽, 0.05 mg/ml; ○, 0.1 mg/ml.

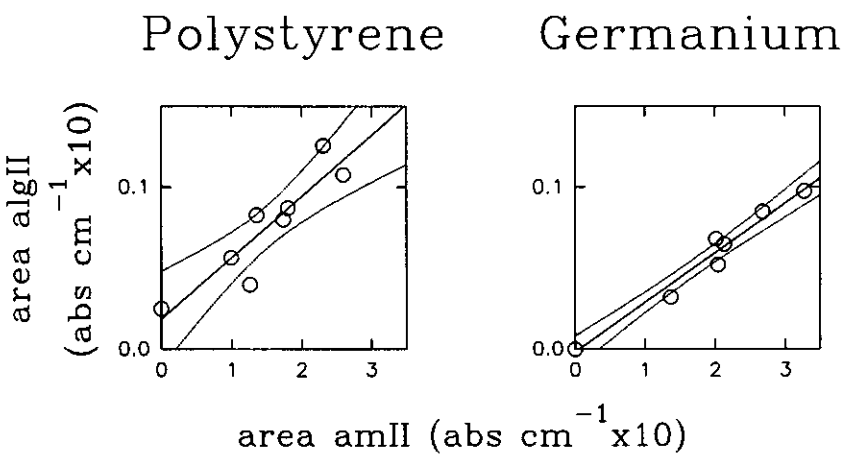

FIG. 11. Area of the alginate band algII versus MAP surface coverage for polystyrene and germanium conditioned with MAP. The curved lines are the 95% confidence intervals for the linear regression (solid line).

polylysine, and APS films originate from a more complex molecular interaction between alginate and protonated amines. Quite complex bonding is possible with divalent cations, e.g., cross-linking of alginate by Ca^{+2} involves coordination to hydroxyl, ring, and glycosidic linkage oxygens (46).

It is possible that a component of the alginate is being selectively, and irreversibly, adsorbed to the surfaces presenting lysine groups. This could account for the differences in spectral features of the adsorbed and bulk alginate components. This component could be an alginate fraction which differs from the bulk of the alginate in mannuronic and guluronic composition and thus incorporates different intramolecular H-bonding interactions, or it could be a polysaccharide contaminant incorporating different monosaccharide units. Spectra of sulfated polysaccharides contain features similar to those presented in Figs. 8a–8c (43). However, the alginate used for our experiments contains only a trace amount of sulfur (0.06%). In addition, the algII band at 965 cm^{-1} which is associated with the component of alginate retained on MAP-conditioned surfaces is conspicuously absent in the transmission spectrum of bulk alginate (Fig. 7a). Since this band is relatively isolated from other alginate bands, a contaminant level of less than 1% should be detectable. Moreover, phosphate or sulfate ions are retained for less than 5 min on polylysine-conditioned germanium after a 30-min exposure, while some gluconic acid (a pyranose ring incorporating a carboxylate moiety) remains after a 120-min rinse period with the synthetic seawater (data not shown).

Alginate and polylysine form a white precipitate in bulk solution, indicating that they cross-link readily in solution through intermolecular bonding. The solution clears at high pH, indicating that these bonds are apparently broken when the lysine groups are deprotonated. This suggests that the bond is ionic in nature. Spectral features which appear in the transmission spectrum of the precipitate formed in the mixture of alginate and polylysine are not identical to those which are present in alginate retained on germanium conditioned with polylysine. Notably the wide band between 1200 and 1300 cm^{-1} is not prominent. The band centered at 1037 cm^{-1} is widened in the mixture, but no distinct shoulder appears at 1054 cm^{-1}. A band is evident at 950 cm^{-1} in the mixture which is not present in pure alginate. (The transmission spectrum of pure polylysine is essentially featureless in the region from 1100 to 900 cm^{-1} (data not shown).) This suggests that bonding in solution between polylysine and alginate differs significantly from bonding at the interface.

4.2. Influence of the Underlying Substratum on Polysaccharide Binding to MAP-Conditioning Films

Our research effort is directed at devising means to characterize proteinaceous conditioning film "stickiness" and to determine if this polysaccharide bonding potential can be modified by the underlying substratum. Technically, this latter task involves identifying some IR spectral feature that originates specifically from a bonding interaction and that can be distinguished in difference spectra containing multiple interfering background signals. The band algII in Fig. 7d is isolated from other alginate bands and from polystyrene bands and is thus suitable for this purpose. Using the empirical relation between the area of this band and surface coverage of MAP as an index for comparison, it appears that the intensity of the interaction between alginate and MAP-conditioned surfaces is similar for germanium and polystyrene substrata (Fig. 11). These substrata differ significantly in surface free energy as well as in chemical nature.

4.3. Significance of the Results for Investigation of Microbial Fouling

We are presently experimenting with different techniques to modify germanium ATR prisms with stable coatings

which confer a variety of surface properties. In this respect, the ability to detect and recognize a bonding interaction between specific moieties on a polysaccharide and an adsorbed protein layer using ATR/FT-IR should serve as a useful tool for further studies. It provides an experimental handle for investigating the influence of various surface properties on the availability of lysine residues of the adsorbed protein layer with respect to polysaccharide binding. In general, these types of studies may lead to insight into the effect of surface properties on protein conformation as it relates to presentation of hydrophilic residues to other biomolecules in the aqueous subphase. In addition, the molecular bonding between acidic bacterial exopolysaccharides, or more generally those incorporating anionic groups, and proteinaceous conditioning films presenting lysine groups may be a significant bonding interaction in particular cases of marine fouling. This is indicated by the effective use of both MAP and polylysine in promoting cell adhesion.

5. SUMMARY

This study was directed at understanding how proteinaceous conditioning films mediate cellular adhesion in marine environments. MAP was chosen as a model conditioning film because of its quality of being "sticky." Binding of alginate to MAP-conditioned substrata was investigated with the rationale that polysaccharides (including acidic polysaccharides) typically connect biofilm cells to each other and to the (conditioned) substratum. In this context, two questions were posed: What are the molecular interactions conferring stickiness to MAP? Can this property be modified by the underlying substratum? Evidence has been presented indicating that lysine residues play a prominent role in binding of alginate to MAP. One reasonable interpretation of the results is that the initial adsorption reaction is electrostatically driven, but that the binding of alginate to MAP is more complex than electrostatic bonding between the protonated amines of MAP and the carboxylate ion of alginate, involving formation of multiple new intra- or intermolecular bonds. An alternative hypothesis is that MAP promotes binding of a trace polysaccharide component of alginate which differs in monosaccharide unit molecular structure. The empirical relation between the degree of irreversible binding and MAP surface coverage indicates that the strength of the interaction is similar for germanium and polystyrene conditioned with MAP, even though these underlying substrata differ greatly in surface free energy and chemical nature.

ACKNOWLEDGMENTS

This work was supported by the Office of Naval Research Grant N00014-93-1-0168, Cooperative Agreement ECD-8907039 between the National Science Foundation and Montana State University, and Electrical Power Research Institute Grant RP8011-2. We are grateful to Ace Baty for performing the XPS analysis.

REFERENCES

1. Price, T. M., and Rudee, M. L., *in* "Proteins at Interfaces, Physiochemical and Biochemical Studies" (J. L. Brash and T. A. Horbett, Eds.), pp. 49–62. ACS Symposium Series. Am. Chem. Soc., Washington, DC, 1987.
2. Baier, R. E., *in* "Proceedings, Third International Congress on Marine Corrosion and Fouling," pp. 633–639. Natl. Bur. of Standards, Gathersburg, MD, 1972.
3. Baier, R. E., Meyer, A. E., DePalma, V. A., King, R. W., and Fornalik, M. S., *Trans. ASME* **105,** 618 (1983).
4. Loeb, G. I., and Neihof, R. A., *J. Mar. Res.* **35,** 283 (1977).
5. Kristoffersen, A., Rolla, G., Skjorland, K., Glantz, P. O., and Ivarsson, B., *J. Colloid Interface Sci.* **86,** 196 (1982).
6. Little, B., and Jacobus, J., *Org. Geochem.* **8,** 27 (1985).
7. Chamberlain, A. H. L., *in* "Biofilms: Science and Technology" (L. Melo *et al.*, Eds.), pp. 59–67. Kluwer Academic, Dordrecht, The Netherlands, 1992.
8. Corpe, W. A., *Dev. Ind. Microbiol.* **11,** 402 (1970).
9. Fletcher, M., and Floodgate, G. D., *J. Gen. Microbiol.* **74,** 325 (1973).
10. Characklis, W. G., and Cooksey, K. E., *Adv. Appl. Microbiol.* **29,** 93 (1983).
11. Allison, D. G., and Sutherland, I. W., *J. Gen. Microbiol.* **133,** 1319 (1987).
12. Cooksey, K. E., *in* "Biofilms: Science and Technology" (L. Melo *et al.*, Eds.), pp. 137–147. Kluwer Academic, Dordrecht, The Netherlands, 1992.
13. Waite, J. H., and Tanzer, M. L., *Science* **212,** 1038 (1981).
14. Waite, J. H., *Int. J. Adhes. Adhes.* **7,** 9 (1987).
15. Waite, J. H., *Int. J. Biol. Macromol.* **12,** 139 (1990).
16. MAP is sold commercially as a cell adhesive under the name Cell-Tak by Collaborative Biomedical Products, a division of Becton–Dickinson Labware, Bedford, MA. According to a personal communication from the supplier Cell-Tak has been reported to enhance attachment of *Escherichia coli, Staphylococcus aureus, Saccharomyces cerevisiae, Naegleria, Streptococcus sanguis,* and *Dictyostelium discoideum.*
17. Benedict, C. V., and Picciano, P. T., *in* "Adhesives from Renewable Resources" (R. W. Hemingway *et al.*, Eds.), pp. 466–483. ACS Symposium Series. Am. Chem. Soc., Washington, DC, 1987.
18. Notter, M. F., *Exp. Cell Res.* **177,** 237 (1988).
19. Nagy, P. I., Patel, H. C., Dreyer, W., and Hopfinger, A. J., *Int. J. Pep. Protein Res.* **38,** 84 (1991).
20. Williams, T., Marumo, K., Waite, J. H., and Henkens, R. W., *Arch. Biochem. Biophys.* **269,** 415 (1989).
21. Mozes, N., and Rouxhet, P. G., *in* "Biofilms—Science and Technology," (L. F. Melo *et al.*, Eds.), pp. 69–85. Kluwer Academic, Dordrecht, The Netherlands, 1992.
22. Goding, J. W., "Monoclonal Antibodies: Principles and Practice," p. 162. Academic Press, London, 1983.
23. Cotrell, I. W., and Kovacs, P., *in* "Food Colloids" (H. D. Graham, Ed.), pp. 438–463. AVI, Westport, CT, 1977.
24. Evans, L. R., and Linker A., *J. Bacteriol.* **116,** 915 (1973).
25. Christensen, B. E., Kjorbakken, J., and Smidsrod, O., *Appl. Environ. Microbiol.* **30,** 837 (1985).
26. Uhlinger, D. J., and White, D. C., *Appl. Environ. Microbiol.* **45,** 64 (1983).
27. Sutherland, I. W., *in* "Microbial Adhesion to Surfaces" (R. C. W. Berkeley, J. M. Lynch, J. Melling, and B. Vincent, Eds.), pp. 329–338. Ellis Horwood, Chichester, UK, 1980.
28. Christensen, B. E., *J. Biotechnol.* **10,** 181 (1989).
29. Ishida, K. P., and Griffiths, P. R., *J. Colloid Interface Sci.* **160,** 190 (1993).
30. Lowry, O. H., Rosenbrough, N. J., Farr, A. L., and Randal, R. J., *J. Biol. Chem.* **193,** 265 (1951).

31. Naval aircraft factory process specification PS-1 for synthetic seawater; Naval Department Specification 44T27b, dated July 1, 1940; similar recipes have been published elsewhere; see, e.g., Lyman, J., and Fleming, R. H., *J. Mar. Res.* **3,** 134 (1940).
32. Paz, M. A., Fluckinger, R., Boak, A., Kagan, H., and Gallop, P. M., *J. Biol. Chem.* **266,** 689 (1991).
33. Arnow, L. E., *J. Biol. Chem.* **118,** 531 (1937).
34. Waite, J. H., and Benedict, C. V., *Methods Enzymol.* **107,** 397 (1984).
35. Waite, J. H., *Methods Enzymol.*, in press, 1995.
36. Waite, J. H., Housley, T. J., and Tanzer, M. L., *Biochemistry* **24,** 5010 (1985).
37. Dousseau, F., Therien, M., Pezolet, M., *Appl. Spectrosc.* **43,** 538 (1989).
38. Fink, D. J., Hutson, T. B., Chittur, K. K., and Gendreau, R. M., *Anal. Biochem.* **165,** 147 (1987).
39. Knutzen, K., and Lyman, D. J., *in* "Surface and Interfacial Aspects of Biomedical Polymers. Vol. 1. Surface Chemistry and Physics" (J. D. Andrade, Ed.), pp. 197–247. Plenum Press, New York, 1985.
40. Olivieri, M. P., Loomis, R. E., Meyer, A. E., and Baier, R. E., *J. Adhes. Sci. Technol.* **4,** 197 (1990).
41. Olivieri, M. P., Loomis, R. E., and Baier, R. E., *Biomaterials* **13,** 1000 (1992).
42. Cael, J. J., Koenig, J. L., and Blackwell, J., *Biopolymers* **14,** 1885 (1975).
43. Parker, F. S., *in* "Applications of Infrared, Raman, Resonance Raman in Biochemistry, pp. 315–347. Plenum Press, New York, 1983.
44. Waite, J. H., *Chem. Ind. (London)*, 607 (1991).
45. Peters, T., Jr., *Adv. Protein Chem.* **37,** 161 (1985).
46. Smidsrod, O., and Skjak-Braek, G., *TIBTECH* **8,** 71 (1990).